NJC

New Journal of Chemistry

A journal for new directions in chemistry

Accepted Manuscript

This article can be cited before page numbers have been issued, to do this please use: P. Lu, T. Mingliang, E. Hondo, L. Gapu Chizema, C. Du, Q. Ma, S. Mo, C. Lu and N. Tsubaki, *New J. Chem.*, 2020, DOI: 10.1039/D0NJ00907E.

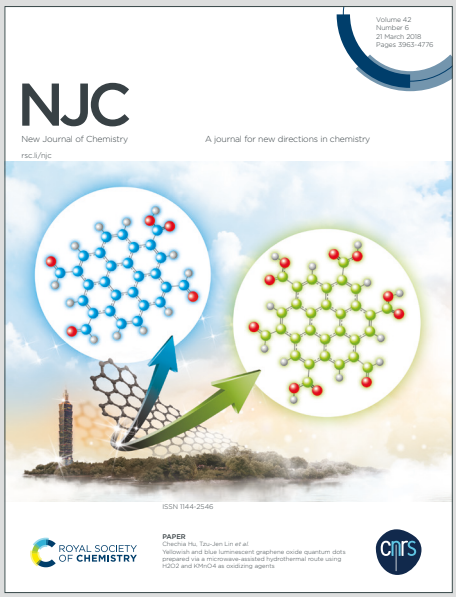

This is an Accepted Manuscript, which has been through the Royal Society of Chemistry peer review process and has been accepted for publication.

Accepted Manuscripts are published online shortly after acceptance, before technical editing, formatting and proof reading. Using this free service, authors can make their results available to the community, in citable form, before we publish the edited article. We will replace this Accepted Manuscript with the edited and formatted Advance Article as soon as it is available.

You can find more information about Accepted Manuscripts in the Information for Authors.

Please note that technical editing may introduce minor changes to the text and/or graphics, which may alter content. The journal's standard Terms & Conditions and the Ethical guidelines still apply. In no event shall the Royal Society of Chemistry be held responsible for any errors or omissions in this Accepted Manuscript or any consequences arising from the use of any information it contains.

View Article Online
DOI: 10.1039/D0NJ00907E

Hydrogenation of CO_2 to LPG over CuZnZr/MeSAPO-34 Catalyst

Mingliang Tong[a+], Emmerson Hondo[a+], Linet Gapu Chizema[a], Ce Du[a,c], Qingxiang Ma[b], Shuting Mo[a], Chengxue Lu[a], Peng Lu[a,b]*, Noritatsu Tsubaki [d]*

a Zhejiang Provincial Key Lab for Chem. & Bio. Processing Technology of Farm Product, School of Biological and Chemical Engineering, Zhejiang University of Science and Technology, Hangzhou, 310023, PR China

b State Key Laboratory Cultivation Base of Natural Gas Conversion, Ningxia University, Yinchuan 750021, PR China

c Department of Applied Chemistry, School of Engineering, University of Toyama, Gofuku 3190, Toyama 930-8555, Japan

[+]These authors have equal contribution

*Corresponding authors

Email: lvpeng0830@zust.edu.cn (Peng Lu)

Email: tsubaki@eng.u-toyama.ac.jp (Noritatsu Tsubaki)

Abstract

The utilization of CO_2 to synthesize environmentally begnin liquid fuels offers a solution to replacing depleting petroleum resources. Herein, a ternary CuZnZr (CZZ) metal oxide catalyst and a SAPO-34 zeolite was synthesized by co-precipitation and hydrothermal synthesis, respectively. Different metals were impregnated into the latter to obtain MeSAPO-34 (Me= Mn, Zn and Zr). A granule mixture of CZZ and MeSAPO-34 components (CZZ/MeSAPO-34 catalyst) was then effectively utilized in a tandem catalytic process for one-step CO_2 hydrogenation to liquefied petroleum gas (LPG). The CZZ/MeSAPO-34 catalysts were characterized by XRD, H_2-TPR, BET, SEM-EDS and NH_3-TPD techniques. SEM-EDS and XRD results indicated that an appropriate amount of Zr metal loading induced minimum zeolite framework collapse compared to a similar amount of Mn and Zn, which was more favorable for higher activity. In addition, NH_3-TPD results revealed that the acidity of SAPO-34 could be altered after impregnation with different metals in varied quantities. Tuning the acid density and strength, together with adjusting the CZZ to MeSAPO-34 weight ratio, had a collectively critical effect on LPG selectivity. An effective hydrogenation microenvironment which favors lower alkane formation (C_3-C_4) was enhanced after the acidity of molecular sieve was tuned. LPG selectivity could reach 86% over CZZ/5%ZrSAPO-34 catalyst at 2 MPa, 350 ^oC, W/F of 6, H_2/CO_2 of 3 and weight ratio of 1.

Keywords: CO_2; CZZ; Hydrogenation; LPG; MeSAPO-34

1. Introduction

Global energy crisis escalated by gradual crude oil depletion and increase in population has driven current research towards synthesis of high value hydrocarbon fuels from cheap and abundant one-carbon (C1) feed stocks such as CO_2 and CO. The accumulation of anthropogenic CO_2 in the atmosphere has also given rise to serious environmental concerns such as climate changes. To date, viable strategies namely carbon capture and utilization (CCU) have been developed to minimize direct CO_2 emission into the atmosphere. There are quite a number of existing technologies in

CCU, involving the conversion of CO_2 to C1 and short-chain products such as CH_4, HCOOH and CH_3OH.[1-3]

Catalytic CO_2 hydrogenation to liquid petroleum gas (LPG) also provides a sustainable route for production of clean fuel and diminution of carbon emissions. Liquefied petroleum gas is a mixture of propane and butane which is mostly obtained from crude oil refining and natural gas. LPG is comparable to petrol or diesel in terms of engine performance and maintenance.[4, 5] It has environmentally benign characteristics, thus, it can be conveniently used in the household and industry as a substitute for other petroleum-based fuels. Additionally, LPG can be easily converted, stored and transported as a liquid phase. Therefore, it is a worthy target product for CO_2 conversion.

There are two major catalytic approaches to transformation of CO_2 to LPG. The first route involves the traditional Fischer Tropsch synthesis (FTS) route which is combined with the reverse water–gas shift (RWGS) reaction (RWGS-FT) using modified FT catalysts.[6, 7] RWGS reaction produces CO from CO_2 hydrogenation (eqn 1) which then proceeds via FT route (eqn 2) to produce light olefins and paraffins (eqn 3). FTS is a process that produces hydrocarbons through syngas (CO/H_2) transformation over FT catalysts, namely Fe, Co, Ru and Ni. However, the selectivity of any particular hydrocarbon species is restricted by Anderson-Schulz-Flory (ASF) law of distribution, unless the catalysts are modified. Another inherent drawback of this pathway is the thermodynamic feasibility of the two reactions at different temperature ranges. RWGS reaction is endothermic; therefore, it is thermodynamically favored at higher temperatures, whereas FTS reaction is exothermic and requires a lower temperature.

$$H_2 + CO_2 \rightarrow CO + H_2O \quad (1)$$

$$2nH_2 + nCO \rightarrow C_nH_{2n} + nH_2O \quad (2)$$

$$(2n + 1)H_2 + nCO \rightarrow C_nH_{2n+2} + nH_2O \quad (3)$$

The second route, a catalytic approach different from FTS, involves CO_2 hydrogenation to light alkanes over a hybrid catalyst consisting of a methanol

synthesis catalyst and a zeolite.[8] The light alkanes can be specifically synthesized over bifunctional catalysts via reaction intermediates such as methanol and dimethyl ether followed by chain growth into C_3 and C_4 hydrocarbons.

Previous reports have concurred that metallic Cu facilitates H_2 dissociation reactions and provides hydrogen resource [9-12], and also Zr-modified Cu/Zn catalysts (e.g. CZZ) have commendable activity and good stability for methanol synthesis via CO_2 hydrogenation.[9, 13] It has been realized that Zr improves surface basicity, which could promote CO_2 adsorption [14] and the Cu/ZrO_2 synergy establishes Cu–ZrO_2 interfacial sites [9], which may improve the dissociation of H_2 and spillover of atomic hydrogen.[15] In addition, it has also been reported that an intrinsic interaction between ZnO and CuO species can enhance particle dispersion, where ZnO particles function as spacers amongst Cu particles hindering them from sintering.[16] ZnO can be viewed as a structure directing support which bridles morphology, activity and dispersion of metal particles.[10, 17] Wang et al., [9] regarded the ZnO-ZrO_2 interface as the active sites for CO_2 adsorption and conversion, whereas metallic Cu facilitated dissociative chemisorption of H_2 according to density functional theory (DFT) calculations and in-situ diffuse reflectance infrared fourier transform spectroscopy (DRIFTS) measurements.

It is well acknowledged that light olefins can be synthesized from methanol or dimethyl ether (DME) over SAPO-34 zeolite owing to its shape selectiveness (small eight-ring pore size=0.38 nm). Generally, in order to extend zeolite catalysts life time and improve stability, modification with metals has been employed.[18-20] Recently, studies have been conducted where cerium, zirconium [20], and zinc [21] were used to tune some SAPO-34 properties. Apart from stability enhancement, the metal incorporation also modified the zeolite acid density for higher product selectivity.

In this work, the granule mixed combination of a ternary metallic CZZ catalyst and modified zeolite catalyst (5%ZrSAPO-34) were found suitable for the series reaction of converting CO_2 to LPG. Critical reaction intermediates such as light olefins could undergo secondary hydrogenation due to enhanced hydrogen transfer reactions, resulting in an escalated LPG formation. The results revealed that the

multifunctional catalyst has remarkable activity and selectivity for C_3-C_4-rich hydrocarbons. The process of hydrocarbon formation and the product distribution have been discussed in detail in this work.

2. Experimental Section

2.1 Catalyst Preparation

CuOZnOZrO$_2$ catalyst

Ternary oxide catalyst with Cu/Zn/Zr molar ratio of 5:3:1 was prepared by traditional co-precipitation method. Firstly, $Cu(NO_3)_2{\cdot}3H_2O$, $Zn(NO_3)_2{\cdot}6H_2O$ and $Zr(NO_3)_4{\cdot}5H_2O$ were dissolved in deionized water to make a mixed salt solution (solution A) with total metal ion concentration of 1 mol/L. Solution A was then stirred for 1 h at 60 ^oC. An excess amount of Na_2CO_3 was dissolved in deionized water to make solution B, which was added dropwise to solution A until the pH value reached 8. During precipitation, the mixture was kept under vigorous stirring at 80 ^oC, for 2 h, then subsequently aged at room temperature. Hereafter, the obtained precipitate was separated by centrifugation and washed for at least 5 times with deionized water. Drying process was done at 120 ^oC for 3 h followed by calcination in air at 500 ^oC for 5 h. The fresh CZZ catalyst was granulated into pellet size of 20-40 mesh.

MeSAPO-34 catalyst

SAPO-34 molecular sieve was prepared following the hydrothermal synthesis technique.[21] Modified SAPO-34 was then prepared by ultrasonic-impregnation method. The as-synthesized SAPO-34 (2 g) was weighed into an evaporating dish and a certain amount of either $Zn(NO_3)_2{\cdot}6H_2O$, $Zr(NO_3)_4{\cdot}5H_2O$, or $Mn(NO_3)_2$ solution was loaded into the SAPO-34 under ultrasonic agitation for 30 min. The modified zeolite, identified as Me/SAPO-34 (Me=Zn, Zr, Mn) was placed in a vacuum chamber for 10 mins before drying in air at 60 ^oC, followed by calcination at 500 ^oC for 4 h in air. Me/SAPO-34 catalysts were also separately granulated into 20-40 mesh size prior mixing with CZZ catalyst in varying weight ratios. The most suitable metal additive for zeolite modification (denoted as *x*MeSAPO-34 where *x*=1wt%, 3wt%, 5wt%, 7wt% and 10wt%) was further varied to investigate the most appropriate amount. The

View Article Online
DOI: 10.1039/D0NJ00907E

preparation steps are summarized in Scheme 1.

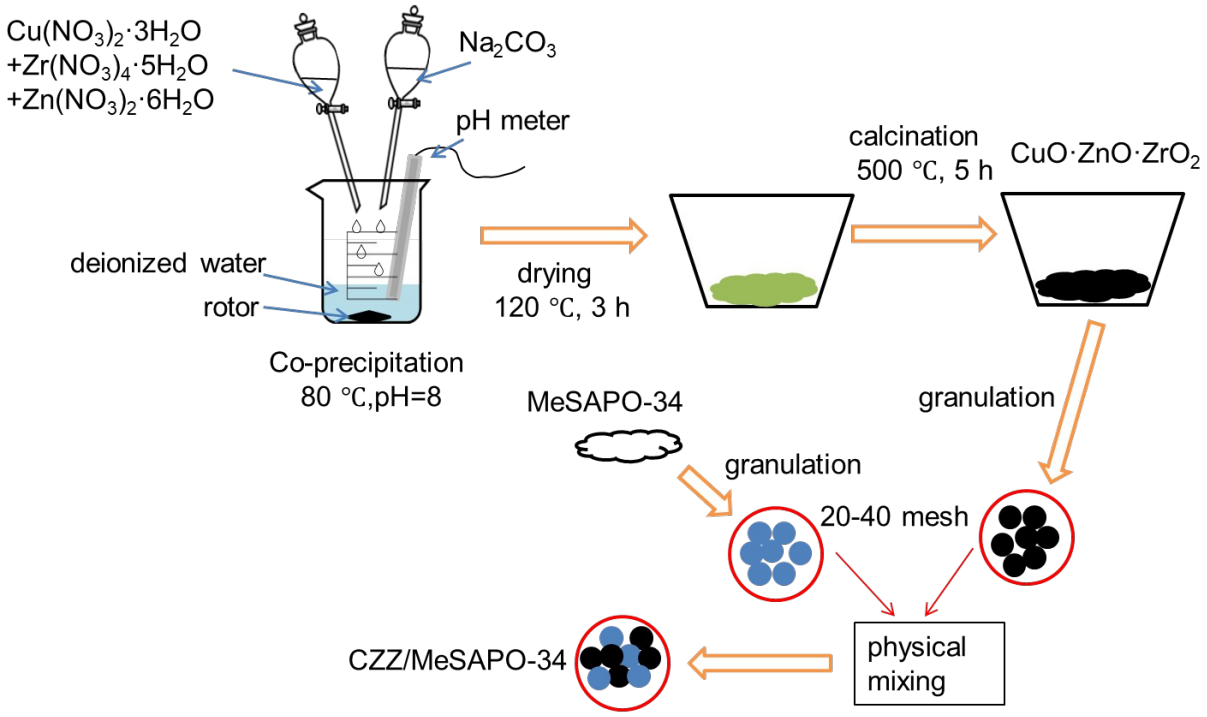

Scheme 1. Schematic representation of the CZZ/MeSAPO-34 catalyst preparation process.

2.2 Catalysts characterization

Temperature programmed reduction (H_2-TPR) and NH_3 temperature programmed desorption (NH_3-TPD) were performed on a BELCAT-B3 (BEL, Japan) apparatus furnished with a thermal conductivity detector (TCD).

N_2 physisorption was carried out on an automatic gas adsorption system (Micromeritics, ASAP 2460). Specific surface area and pore sizes of the catalysts were analyzed by Brunauer–Emmett–Teller (BET) and Barrett–Joyner–Halenda (BJH) methods respectively.

X-ray diffraction (XRD) patterns were determined with RINT 2400 diffractometer using Cu Kα radiation source (λ=1.54 Å, scanning rate of 4° min^{-1} in the range of 5°-80°, at 40 kV and 40 mA.).

The surface morphology of all catalysts was obtained by a scanning electron microscope (SEM, JEOL JSM6360LV). The elemental content of the various catalysts was determined by the energy dispersive spectrometer (EDS, JED 2300) connected to

View Article Online
DOI: 10.1039/D0NJ00907E

the SEM apparatus.

2.3 Catalytic activity testing

LPG synthesis reaction was performed in a continuous flow fixed-bed stainless steel tubular reactor (i.d: 6.8 mm). 1 g of catalyst, mixed with a certain amount of inert SiO_2 to prevent hot spot generation, was loaded by granular stacking into the reactor and held in position by quartz wool. All samples were reduced in pure H_2 for 4 h (280 ^oC, GHSV=4800 h^{-1} at atmospheric pressure) prior reaction. Synthesis gas (H_2/CO_2=3) was used as feed gas under reaction conditions of 350 ^oC, GHSV=4200 h^{-1} and 2 MPa. Feed gas flow was controlled by a mass flow controller. Catalytic performance was discussed after 360 mins of reaction. The gaseous products were analyzed online by a gas chromatograph consisting of a flame-ionization (FID) detector equipped with an Agilent HP-Plot/Q column. The gaseous effluent (CO, CO_2 and CH_4) was quantitatively analyzed using an online gas chromatograph comprising a thermal conductivity detector (TCD) furnished with a TDX-01 column.

Calculations for hydrocarbons distribution was on a molar carbon basis. CO_2 conversion and product selectivity were calculated by the following formulae:

$$x_{co2}\% = \frac{F_{in}C_{co2,\,in} - F_{out}C_{co2,\,out}}{F_{in}C_{co2,\,in}} \times 100\%$$

$$s_i\% = \frac{n_i C_{i,\,out}}{\sum n_i C_{i,\,out}} \times 100\%$$

where x_{co2}%: CO_2 conversion, F_{in}: inlet feed gas flow, $C_{co2,in}$: inlet CO_2 molar content, F_{out}: outlet gas flow, $C_{co2,out}$: outlet CO_2 molar content, s_i%: selectivity of i component, n_i: number of carbon atoms of i component in product and $C_{i,out}$: component i molar content of gas outlet.

View Article Online
DOI: 10.1039/D0NJ00907E

3. Results and Discussion

3.1 XRD Patterns

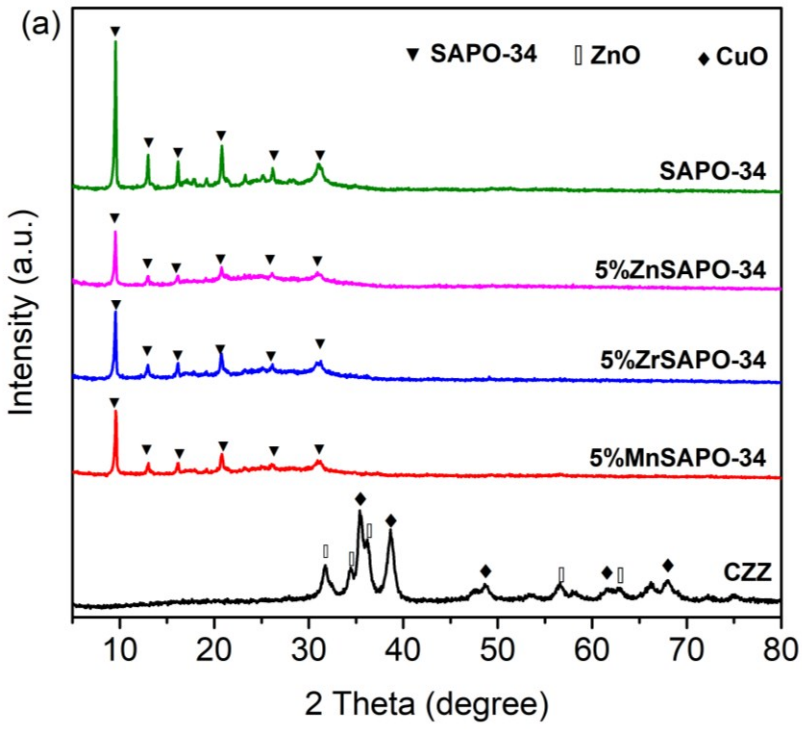

Fig. 1 a. XRD patterns of the fresh CZZ, SAPO-34 and 5%MeSAPO-34 samples.

Fig. 1 shows characteristic XRD diffractions for Cu/Zn/Zr and MeSAPO-34 catalysts. For CZZ, the peaks for CuO appeared at 2θ=35°, 38.6°, 48.7°, 61°, and 68°, and ZnO at 2θ= 34.5°, 36.2°, 56.5° and 62.9°, as presented in Fig. 1 a. There were no peaks assignable to ZrO_2, possibly because it existed in a microcrystalline or amorphous state in the ternary oxide catalyst. The hydrothermally synthesized SAPO-34 zeolite exhibited diffraction peaks at 2θ=9.5°, 12.8°, 16.2°, 20.8° and 31.2° [22-24] corresponding to JCPDS number 01-087-1527, demonstrating that the characteristic chabazite structure was successfully constructed. The distinctive zeolite peaks were inherited into MeSAPO-34 (Me= Zn, Zr, Mn) though with slightly weaker intensities, marginally broadened, they indicate an efficacious impregnation procedure of the different metal ions into SAPO-34 microstructure. Fig. 1 b shows that the intensity of SAPO-34 characteristic peaks decreased with increase in Zr metal content. Recent reports have indicated that addition of high amounts Zr into the molecular sieve results in deposition of its oxides in the channels or crystal outer surface,

leading to a smooth zeolite crystal surface, hence reduced crystallinity. [20, 25] At 10wt% Zr content (10%ZrSAPO-34), characteristic zeolite peak intensities were lowest, which further reveals that high zirconia loading amount reduces crystallinity of SAPO-34.

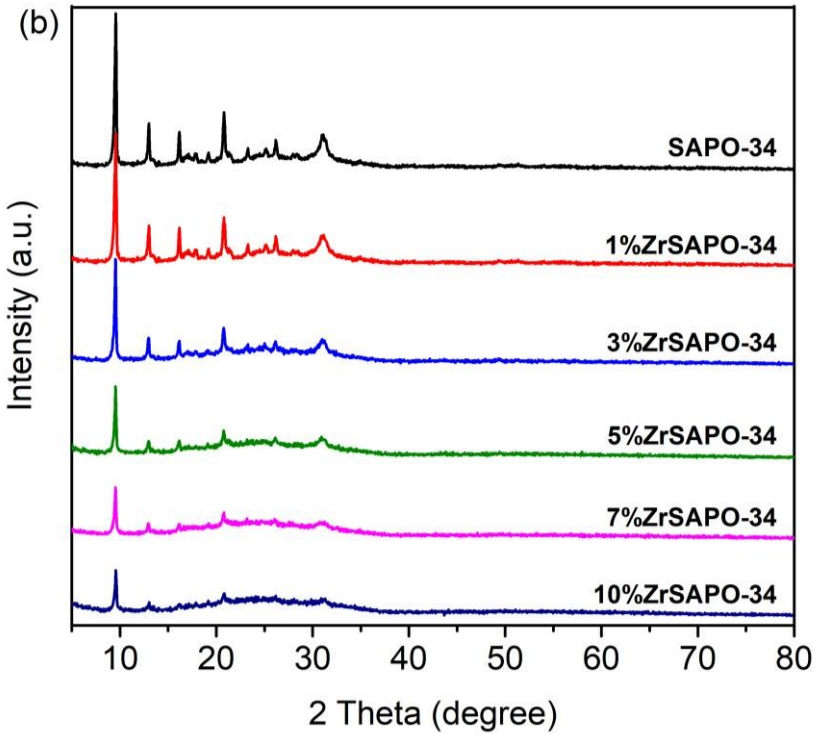

Fig. 1 b. XRD patterns of the fresh *x*ZrSAPO-34 samples

3.2 NH_3-TPD

As displayed in Fig. 2, an almost flat NH_3 desorption profile was observed for CZZ catalyst. The remaining catalysts, denoted as MeSAPO-34 showed desorption peaks with a similar trend, derived from pristine SAPO-34, each with two peaks attributed to weak (hydroxyl groups bound to defect Si−OH, Al−OH and P−OH sites) and strong (hydroxyl groups bound to Si−OH−Al sites) acid sites.[25, 26] There was a slight backward peak shift to a lower temperature observed for 5%MnSAPO-34 and a near-complete degeneration of the strong acid sites for 5%ZnSAPO-34, both attributed to a change in ionic composition of the zeolite after impregnation. Furthermore, weak and strong acid site peaks with closer resemblance to pristine zeolite, but with slightly lower intensities and marginally shifted to lower temperatures, were observed on 5%ZrSAPO-34.

In addition, Table 1 shows the total amount of acid sites in the order of SAPO-34 > 5%MnSAPO-34 > 5%ZnSAPO-34 > 5%ZrSAPO-34, indicating that Zr ions had the ability not only to easily substitute H^+ ions, but to also quickly orientate to the zeolite ionic structure. Table 1 also reveals a sharp decline of weak acid sites in 5%ZrSAPO-34 (0.36 $mmol \cdot g^{-1}$). This could have been because of external surface deposition of ZrO_2 on SAPO-34, covering some of the external acid sites of the zeolite. Because of this phenomenon, it could be deduced that incorporation of an appropriate amount zirconium ions in the molecular sieve ionic environment, yielded a better interaction and controlled effect on the zeolite acidity, thereby making this metal more favorable for enhancing catalytic stability and performance. Acidity analysis of different Zr compositions in SAPO-34 was displayed in Fig. S1 and Table S1.

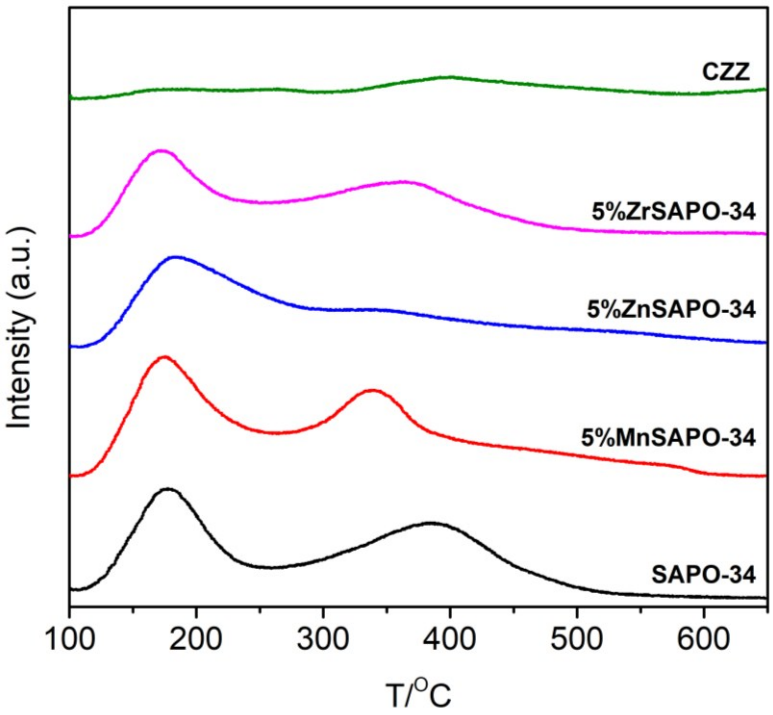

Fig. 2. NH_3-TPD profiles of the fresh CZZ, SAPO-34 and 5%MeSAPO-34 catalysts

View Article Online
DOI: 10.1039/D0NJ00907E

Table 1. Acidity properties of as-synthesized catalysts

Catalysts	Weak acid		Strong acid		Total amount (mmol·g^{-1})
	Temperature (°C)	Acid amount (mmol·g^{-1})	Temperature (°C)	Acid amount (mmol·g^{-1})	
CZZ	-	-	-	-	-
SAPO-34	177	0.68	389	0.51	1.19
5%ZnSAPO-34	186	0.62	400	0.03	0.65
5%ZrSAPO-34	176	0.36	368	0.18	0.54
5%MnSAPO-34	175	0.59	340	0.26	0.85

3.3 H_2-TPR

As shown in Fig. 3, H_2-TPR analysis was used to investigate the hydrogen consumption of a series of catalysts. Both ZnO and ZrO_2 are not reducible within the region experimented, then it becomes obvious that all the reduction peaks are associated to CuO specie [11, 27]. The peaks for CZZ/SAPO-34 exhibited a somewhat subtle shift towards higher reduction temperatures. The same observation was realized for CZZ/*x*MeSAPO-34, which could suggest that the mixture of the two components assumed a mutual interaction which in turn slightly enhanced the surface adsorption of H_2, resulting in the slightly higher reduction temperature (Fig. 3, S2). In essence, the reduction region (200-300 °C) already ascribed to the reduction of CuO species in all catalysts, was maintained.

View Article Online
DOI: 10.1039/D0NJ00907E

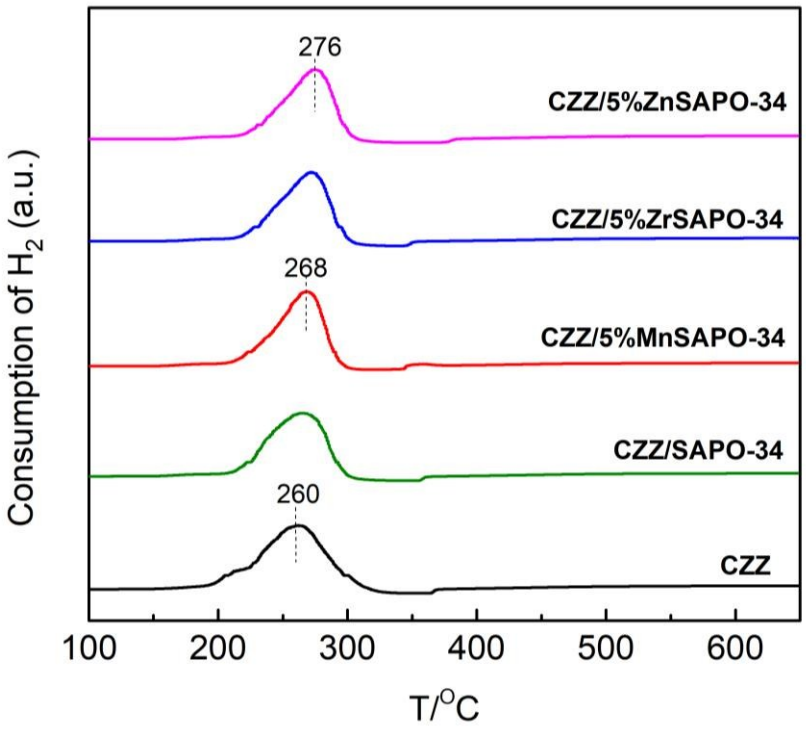

Fig. 3. H_2-TPR profiles of the catalysts

3.4 N_2 adsorption and desorption

In Fig. 4, SAPO-34 and MeSAPO-34 displayed similar N_2 adsorption-desorption isotherms, with strong adsorption observed at relatively low pressures, denoting mostly microporous structures. A series of *x*ZrSAPO-34 (*x*=1, 3, 7, 10wt%) samples also displayed similar isotherms as shown in Fig. S3. However, CZZ catalyst exhibited type IV isotherms with an H3 hysteresis loop (IUPAC catalogue), occurring from P/P_0=0.4 to 1.0, which indicates that its pore structure was mainly mesoporous. Additionally, textural properties of the as-prepared catalysts are shown in Table 2 and Table S2. SAPO-34 possessed the largest surface area (420 m^2/g). On incorporating Mn, Zn or Zr (MeSAPO-34), relative surface areas and pore volumes were significantly reduced. This could be ascribed to the clogging effect of some metal particles on the surface or on the small zeolite pores during the impregnation procedure. The result confirms a possible proposed reason why the relative crystallinity was reduced on modified zeolite structures from the corresponding XRD profiles.

View Article Online
DOI: 10.1039/D0NJ00907E

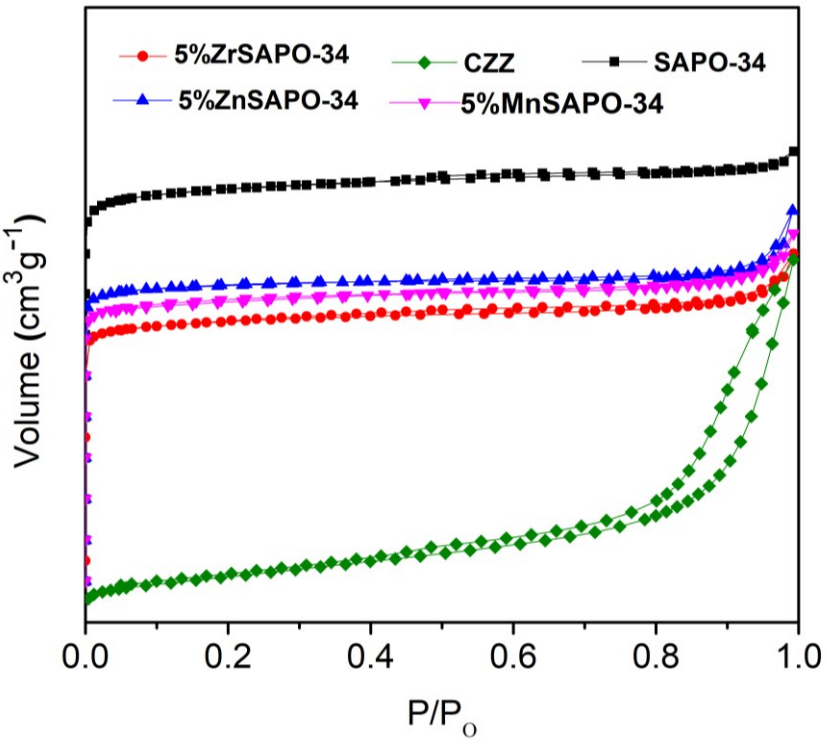

Fig. 4. N_2 adsorption-desorption isotherms of the catalysts

Table 2. Textural properties of the catalysts

Catalysts	BET (m^2g^{-1})	Total pore volume ($cm^{-3}g^{-1}$)
CZZ	41	0.136
SAPO-34	420	0.252
5%ZnSAPO-34	248	0.125
5%ZrSAPO-34	222	0.137
5%MnSAPO-34	238	0.131

3.5 Morphology of catalysts

Fig. 5 shows SEM images of the synthesized CZZ, SAPO-34 and 5%MeSAPO-34 catalysts. CZZ catalyst revealed irregular shaped particles of various sizes. As expected, the as-synthesized SAPO-34 zeolite exhibited fairly uniform sized, cubic shaped granules related to its characteristic CHA structure. SAPO-34 impregnated with up to 5wt% Zr had a smooth surface and maintained the firm characteristic shape indicating that the structure of the zeolite remained intact after

modification. Upon further increase in Zr loading, slight alterations in particle sizes and small particle fragments were observed on the surface of the catalyst (Fig. S4). This could be attributed to the incomplete incorporation of Zr component into zeolite structure which was consistent with the intensity reduction in the XRD analysis (Fig. 1b). Furthermore, EDS analysis (Fig. 5 f) proved that the morphology of the final product relied on the successful impregnation of metal into the zeolite surface structure. Quantitative analysis of 5%ZrSAPO-34 SEM images was conducted using ImageJ software and Fig. S5 represents the particle size distribution histogram. The average particle size of the cubic crystals used for the for MTO step in this investigation was approximated to 1.46 µm. Small particle size distribution is an essential attribute for improving the synthesis of desired products with highest selectivity.

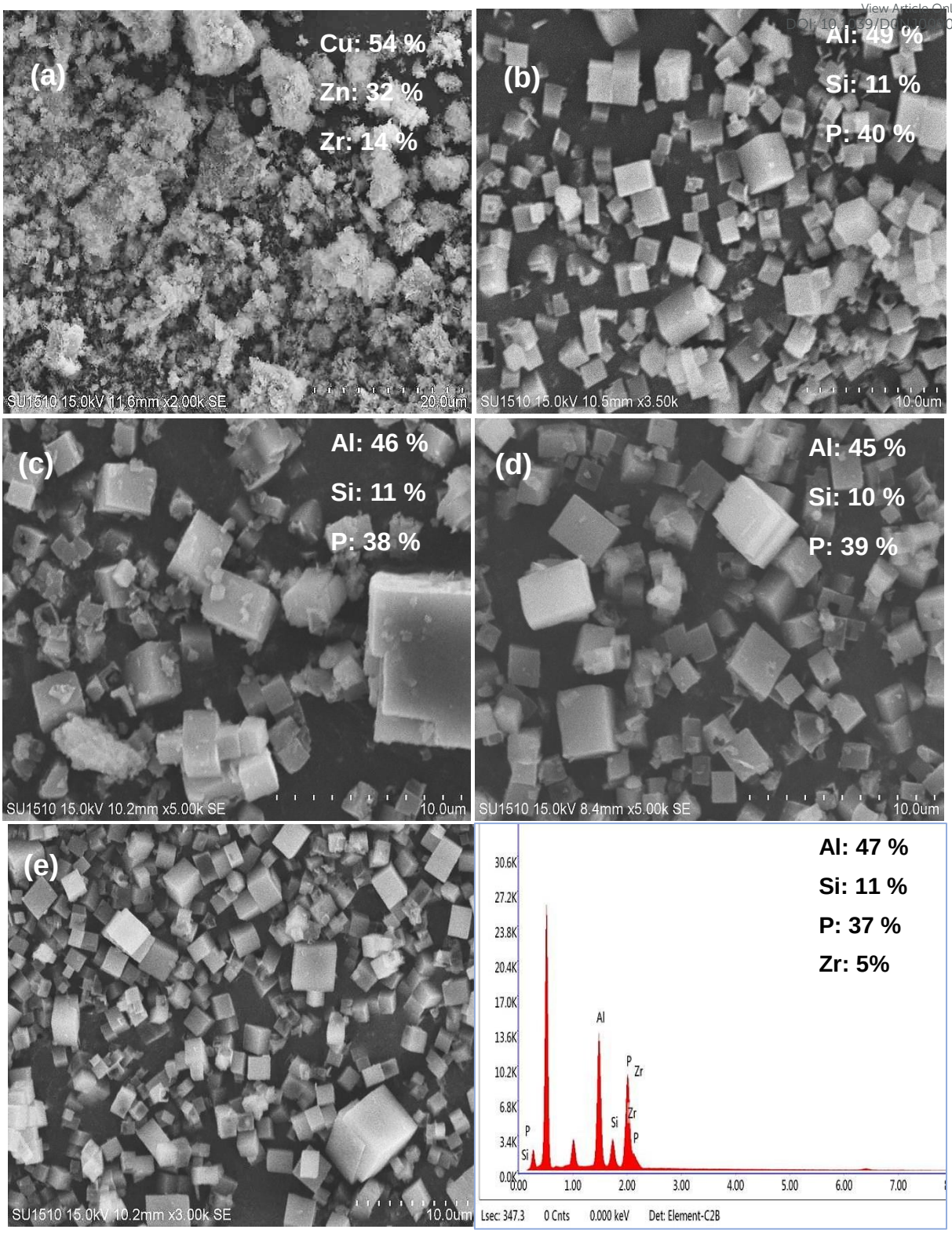

Fig. 5. SEM images (a) CZZ; (b) SAPO-34; (c) 5%MnSAPO-34; (d) 5%ZnSAPO-34; (e) 5%ZrSAPO-34 and (f) EDX analysis of 5%ZrSAPO-34

View Article Online
DOI: 10.1039/D0NJ00907E

3.6 Catalytic activity

The CZZ/*x*MeSAPO-34 catalysts, arranged using the granule stacking method were evaluated for the direct synthesis of LPG from CO_2 hydrogenation and the results are shown in Table 3. Pure Cu-Zn-Zr catalyst and CZZ/SAPO-34 catalyst were also tested under the same reaction conditions as reference catalysts. Synthesis of hydrocarbons from CO_2 hydrogenation over a multifunctional catalyst comprising a methanol synthesis catalyst and modified zeolite generally involves a series of reactions: (1) CO_2 hydrogenation to methanol, (2) methanol dehydration to dimethyl ether (DME) and further dehydration (of generated DME) to olefins over zeolite, (3) olefins hydrogenation to hydrocarbons and (4) reversed water gas shift (RWGS) reaction.[14] The site for methanol synthesis and RWGS reaction ($CO_2 + H_2 \rightarrow CO + H_2O$) was the pure Cu-Zn-Zr catalyst, with CH_4 and CO being the major products as clearly shown in Table 3. These two reactions compete, and a considerably high reaction temperature of 350 ^oC was used as an optimizing adjustment in attaining a better synergy between the two catalysts. CO which mainly dominates the product is recycled to ensure highest productivity. CH_4 selectivity was very high (89.1%) over the ternary oxide, which might have resulted from the direct methanol hydrogenation on metallic sites of CZZ.[28]

Generally, the CO_2 conversion for all catalysts was around 25%. The introduction of a zeolite significantly reduced both methane and CO selectivity. It is highly likely that the synergetic effect established between the hybrid catalysts created a forward thermodynamic driving force which may have depressed the unfavorable RWGS reaction, hence the drop in CO selectivity as observed. Typically, the methanol formed on CZZ catalyst undergoes dehydrogenation to DME and then to hydrocarbons over the modified zeolite, thus molecular sieve catalyst acidity and shape selectivity play a key role in product yield in MTH reaction.

Usually, increasing the strong acid sites of zeolites would improve hydrogen transfer reactions consequently enhancing the transformation of olefins to paraffins. However, the small pore sizes of the SAPO-34 zeolite, to some extent, retards the hydrogen transfer reaction.[29] In this investigation, modification preferably reduced

the acid density of SAPO-34 zeolite which considerably restrained its secondary hydrogenation reaction ability and enhanced the selectivity of olefins. Thus, it is likely that the atomic hydrogen required for LPG formation may have proceeded from the H-spillover of adsorbed hydrogen on Cu under the H_2-rich condition.

A large surface area of SAPO-34 exposed the highest amount of active phase (strong acid sites) and enhanced mass transfer hence a better catalytic activity compared to 5%ZnSAPO-34 and 5%MnSAPO-34. We believe the introduction of Mn and Zn into the zeolite had a somewhat collapsing effect on the overall catalyst framework (Fig. 5) and ionic orientation. LPG selectivity for CZZ/5%ZnSAPO-34 (63.7%) and CZZ/5%MnSAPO-34 (68.1%), was lower probably because both catalysts mixtures contained insufficient acid sites necessary for complete conversion of intermediates to desired product (see acid distribution in NH_3-TPD profile), hence the observed residual DME detected in products.

Table 3. Effect of metal loading on multifunctional catalyst composed of CZZ oxides and 5%MeSAPO-34 for CO_2 hydrogenation to LPG

Catalyst	CO_2 conversion (%)	Selectivity (%)		Hydrocarbons distribution (%)				
		CO	HC	CH_4	DME/ (CH_3OH)	C_2	C_3-C_4	C_{5+}
CZZ	27.9	60.7	39.3	89.1	(1.7)	3.6	5.6	0.0
CZZ/SAPO34	24.0	58.6	41.4	22.8	1.5	0.6	75.1	0.6
CZZ/5%MnSAPO-34	24.8	78.3	21.7	27.1	4.8	0.0	68.1	0.0
CZZ/5%ZnSAPO-34	25.2	78.0	22.0	33.7	0.6	2.0	63.7	0.0
CZZ/5%ZrSAPO-34	25.7	68.4	31.6	9.7	0.0	4.2	86.1	0.0

Reaction conditions: pressure = 2.0 MPa, reaction temperature =350 ºC, GHSV=4200 h^{-1}, C_3^0-C_4^0 paraffins, TOS=360 mins, ratio of CZZ to zeolite = 1, *all hydrocarbon selectivities were calculated CO free.

CZZ/5%ZrSAPO-34 presented the highest C_3-C_4 paraffins selectivity of 86.1%.

The superior performance has been attributed to the availability of an appropriate amount of strong acid sites favorable for LPG selectivity, tuned by metal impregnation. This means there was neither too much acid density (which could cause hydrocarbon cracking or massive coke deposition leading to severe mass transfer limitations), nor too less secondary hydrogenation, which favored target product selectivity.

Furthermore, CZZ/5%ZrSAPO-34 induced minimum zeolite framework collapse as a result of dealumination compared to CZZ/5%MnSAPO-34 and CZZ/5%ZnSAPO-34 catalysts, as indicated by XRD results and SEM images. Rather, an appropriate amount of Zr (≤ 5wt%) is believed to have the ability to facilitate zeolite framework completion [20], maybe because of better interaction capabilities (Fig. 5 e). Such an amount of Zr possibly enhances the ionic microenvironment of the molecular sieve and has a limited collapsing effect. Therefore, there is an appropriate density of acid sites for a more favorable and escalated selective formation of LPG via light olefins transformation.

3.7 Effect of Zr content in zeolite on catalytic performance

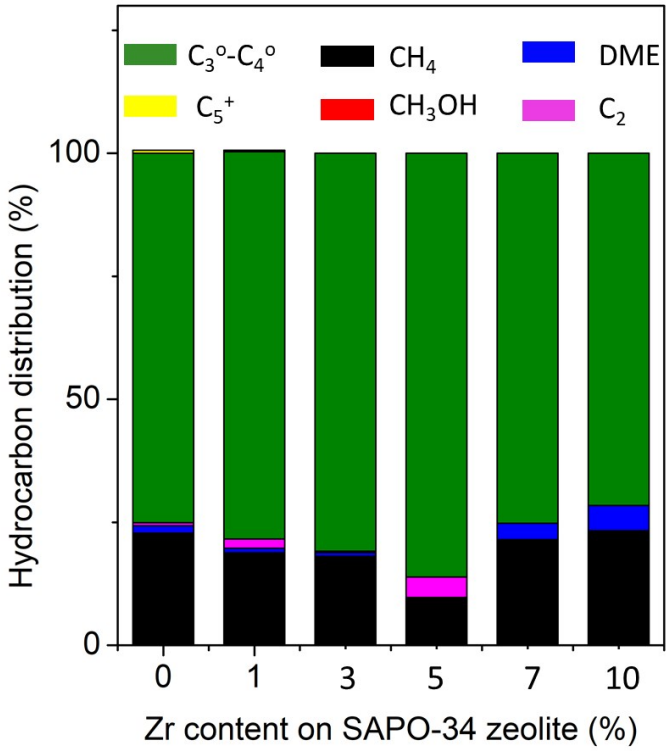

Fig. 6. Effect of zirconia content in SAPO-34 catalysts on hydrocarbon distribution. Reaction conditions: pressure = 2.0 MPa, reaction temperature =350 °C, GHSV=4200

h^{-1}, C_3^0-C_4^0 paraffins, TOS=360 mins, ratio of CZZ to xZrSAPO-34 = 1. * all hydrocarbon selectivities were calculated CO free.

It has been established that during CO_2 conversion to hydrocarbons, it is essential to control the hydrogenation ability and acidity of the zeolite catalysts to attain high selectivity of olefins which will then be hydrogenated to paraffins. As already stated, the introduction of a certain amount of metal-additive had some effect on the crystallinity of SAPO-34 zeolite (Fig. 1 a) as well as a large influence on its surface acidity (Fig. 2, Table 1).

Upon increasing ZrO_2 content from 1 to 3wt%, the CZZ/5%ZrSAPO-34 catalyst exhibited reduced CH_4 and light olefins selectivity whereas paraffins selectivity increased as shown in Fig. 6. The catalyst displayed a highest CO_2 conversion of 25.7% on further increasing Zr content to 5wt%. A significant reduction in methane selectivity (9.7%) and a complete disappearance of intermediate products selectivity, was observed. On the other hand, the selectivity of C_3-C_4 paraffins increased to 86.1%. The CZZ/5%ZrSAPO-34 catalyst possibly provided a sufficient supply of methanol and a hydrogen-rich environment where the synthesized C_2–C_4 olefins unavoidably encountered hydrogen transfer reactions on the metallic sites to generate LPG. Therefore, an increased LPG synthesis was a result of a synergetic parallel reaction phenomenon, where CO_2 conversion to intermediates could be accelerated by intermediates conversion to LPG.

The activity results are in good agreement with, and well supported by the characterization techniques. The NH_3-TPD results indicated that with an increase in Zr content on zeolite catalyst from 1 to 5wt%, the acidity of SAPO-34 was linearly reduced. It has been established that decreasing the acid density of SAPO-34 catalysts improves the selectivity of propylene and higher olefins, formed via the alkene-based reaction route.[30,31]. With further zirconium loading (up to 10wt%), methane selectivity increased (see Table S3), which could be ascribed to DME decomposition over the extra framework ZrO_2 deposited on the outer surface of the zeolite crystals (see Fig. 1b, S4). A decrease in LPG selectivity to 71.6% could be attributed to a

change in the zeolite ionic structure responsible for light olefins synthesis, hence the increase in DME in the products. Furthermore, the diffusion of larger C_{5+} molecules through the narrow pores of the molecular sieves was considerably restricted. Consequently, the C_{5+} hydrocarbons selectivity was negligible (<1%) for CZZ/SAPO composite and 0% for modified CZZ/5%ZrSAPO-34 catalyst. The latter besides a remarkable show of stability (Fig. S6), displayed high selectivity toward C_3-C_4 hydrocarbons because of the suitable acid sites and effective shape selectivity.

3.8 Effect of metal oxide to modified zeolite weight ratio on catalytic performance

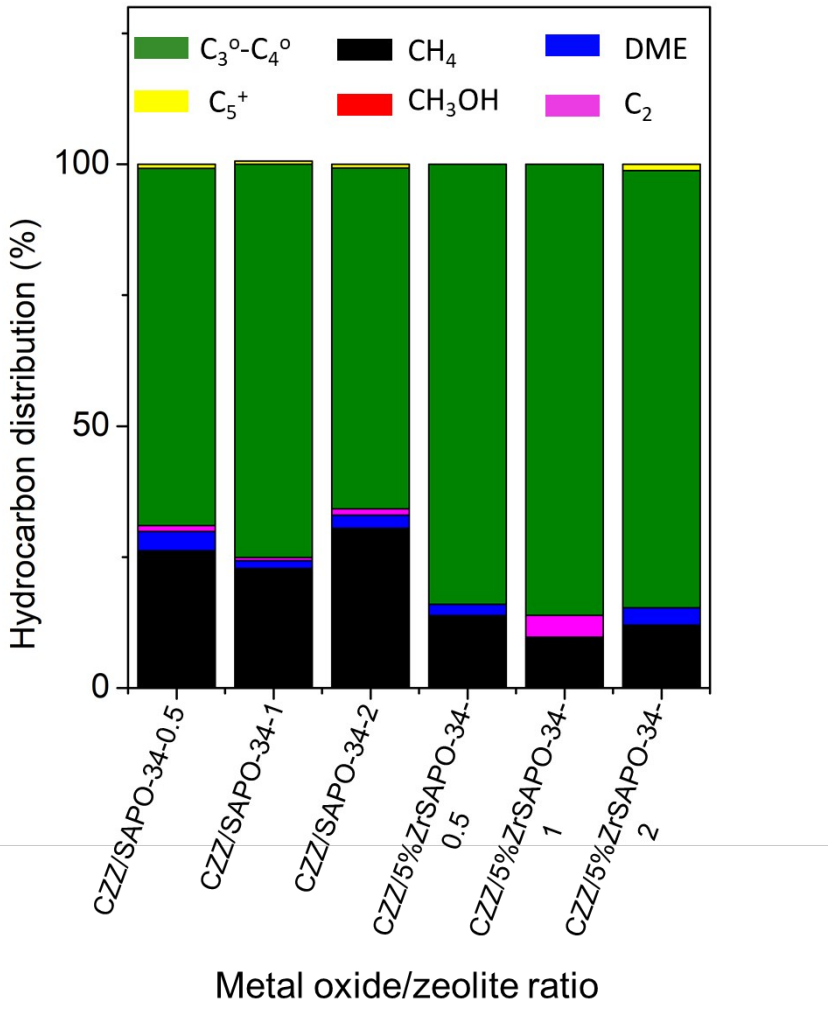

Fig. 7. Effect of metal oxide-to-modified zeolite weight ratio.

Reaction conditions: pressure = 2.0 MPa, reaction temperature =350 °C, GHSV=4200 h^{-1}, C_3^0-C_4^0 paraffins, TOS=360 mins, *all hydrocarbon selectivities were calculated CO free

To further examine the roles played by each component of the composite catalyst, the weight ratio of the metal oxide to molecular sieve was varied. As given in Fig. 7, the steady increase in metal oxide to zeolite (unmodified) ratio from 0.5 to 2, resulted in the increase in CH_4 production to 30.5% and a decrease in the selectivity of LPG to 65.1%. This observation was attributed to the strong hydrogenation ability of the excess CZZ particles under high reaction temperature. CH_4 production was well below 15% for the CZZ/5%ZrSAPO-34, implying that reducing the acid strength of molecular sieve somewhat has some effect on the hydrogenation ability of the CZZ catalyst component. Evidently, the acidic properties of the zeolite exhibited a huge influence on LPG synthesis.

With the increase in weight ratio of CZZ to 5%ZrSAPO-34 from 0.5 to 1, C_3^0-C_4^0 paraffins selectivity increased tremendously (Table S4). At ratio=1, a proportionally abundant amount of methanol was produced which could occupy a large number of acid sites on 5%ZrSAPO-34 to produce a huge quantity of olefins for LPG formation. The observation was associated with the synergetic mechanism of two active sites which facilitated sequential reactions, accelerating transformation of intermediates into product and raw materials into intermediates. However, as the weight ratio of CZZ to 5%ZrSAPO-34 zeolite was further increased, CO_2 conversion and LPG selectivity decreased. An increase in DME in the products distribution was observed, as a short supply of 5%ZrSAPO-34 zeolite could not effectively convert intermediates to LPG in time, possibly due to insufficient reaction sites, thus CO_2 conversion was also reduced. Therefore, the most suitable metal to zeolite weight ratio of 1 was realized for optimal product generation for composite CZZ/5%ZrSAPO-34 catalyst.

4. Conclusions

A composite ternary catalyst comprising CZZ and a modified SAPO-34 molecular sieve were prepared by granule mixing and employed to facilitate LPG direct synthesis from CO_2 hydrogenation. The influence of acid density and strength on product selectivity was probed by modifying the zeolite acid properties, using the facile, low cost ultrasonic-impregnation method. Characterization results clearly indicated that

impregnation of the same amount of different metals induced a weak and strong acid reduction effect, but to different degrees. It was found that the CZZ/5%ZrSAPO-34 catalyst exhibited higher performance for LPG synthesis compared to the unmodified CZZ/SAPO-34 catalyst. The CZZ/5%ZrSAPO-34 catalyst did not only reduce the CH_4 selectivity from 22.8% to 9.7%, but also completely consumed generated intermediates (DME) for increased selectivity toward desired product. CO_2 conversion and LPG selectivity for CZZ/5%ZrSAPO-34 catalyst were highest, 25.7% and 86.1% respectively, at reaction temperature of 350 ^oC, pressure 2.0 MPa, flow GHSV=4200 h^{-1} and an optimized weight ratio CZZ:5%ZrSAPO-34=1. The excellent catalytic performance of CZZ/5%ZrSAPO-34 was mainly attributed to the appropriate acid density and a synergetic relationship established between the metal and modified zeolite components which favored formation of C_3-C_4 olefins that were hydrogenated to LPG. Additionally, this simple and scalable catalyst design inspires the development strategy of new catalysts with better and enhanced product selectivity for improved utilization of CO_2 as a carbon resource.

Acknowledgements

The research work has been funded by the Zhejiang Province Natural Science Foundation (LY19B060001, LY17B060002), Youth Foundation of ZUST (2019QN23) and Foundation of State Key Laboratory of High-efficiency Utilization of Coal and Green Chemical Engineering (2019-KF-21).

Conflict of Interest

The authors have no conflicts to declare.

References

[1] W. Zhou, K. Cheng, J. Kang, C. Zhou, V. Subramanian, Q. Zhang, Y. Wang, New horizon in C1 chemistry: breaking the selectivity limitation in transformation of syngas and hydrogenation of CO_2 into hydrocarbon chemicals and fuels, Chem. Soc. Rev., 48 (2019) 3193-3228.

[2] A. Al-Mamoori, A. Krishnamurthy, A.A. Rownaghi, A. Rezaei, Carbon Capture and Utilization Update, Energy Technol., 5 (2017) 834-849.

[3] S.G. Jadhav, P.D. Vaidya, B.M. Bhanage, J.B. Joshi, Catalytic carbon dioxide hydrogenation to methanol: A review of recent studies, Chem. Eng. Res. Des., 92 (2014) 2557-2567.

[4] A. Simons, S. Nunoo, Liquefied Petroleum Gas as an Alternative Vehicle Fuel in Ghana, Petrol Sci. Technol., 27 (2009) 2223-2233.

[5] C. Du, E. Hondo, L. Gapu Chizema, D. Shen, Q. Ma, X. Yan, S. Mo, P. Lu, N. Tsubaki, LPG Direct Synthesis from Syngas over a Cu/ZnO/ZrO_2/Al_2O_3@H-β Zeolite Capsule Catalyst Prepared by a Facile Physical Method, ChemistrySelect, 5 (2020) 1-7.

[6] Z. He, M. Cui, Q. Qian, J. Zhang, H. Liu, B. Han, Synthesis of liquid fuel via direct hydrogenation of CO_2, PNAS, 116 (2019) 12654-12659.

[7] W. Wang, S. Wang, X. Ma, J. Gong, Recent advances in catalytic hydrogenation of carbon dioxide, Chem. Soc. Rev., 40 (2011) 3703-3727.

[8] C. Li, X. Yuan, K. Fujimoto, Direct synthesis of LPG from carbon dioxide over hybrid catalysts comprising modified methanol synthesis catalyst and β-type zeolite, Appl. Catal. A Gen., 475 (2014) 155-160.

[9] Y. Wang, S. Kattel, W. Gao, K. Li, P. Liu, J.G. Chen, H. Wang, Exploring the ternary interactions in Cu–ZnO–ZrO_2 catalysts for efficient CO_2 hydrogenation to methanol, Nat. Commun., 10 (2019) 1-12.

[10] D. Zhang, H. Yin, R. Zhang, J. Xue, T. Jiang, Gas Phase Hydrogenation of Maleic Anhydride to y-Butyrolactone by Cu–Zn–Ce Catalyst in the Presence of n-Butanol, Catal. Lett., 122 (2008) 176-182.

[11] Z. Lu, H. Yin, A. Wang, J. Hu, W. Xue, H. Yin, S. Liu, Hydrogenation of ethyl acetate to ethanol over Cu/ZnO/MO_x (MO_x = SiO_2, Al_2O_3, and ZrO_2) catalysts, J. Ind Eng Chem., 37 (2016) 208-215.

[12] D. Zhang, H. Yin, C. Ge, J. Xue, T. Jiang, L. Yu, Y. Shen, Selective hydrogenation of maleic anhydride to y-butyrolactone and tetrahydrofuran by Cu–Zn–Zr catalyst in the presence of ethanol, J. Ind Eng Chem., 15 (2009) 537-543.

[13] F. Arena, K. Barbera, G. Italiano, G. Bonura, L. Spadaro, F. Frusteri, Synthesis, characterization and activity pattern of Cu–ZnO/ZrO_2 catalysts in the hydrogenation of carbon dioxide to methanol, J. Catal., 249 (2007) 185-194.

[14] G. Bonura, M. Cordaro, C. Cannilla, F. Arena, F. Frusteri, The changing nature of the active site of Cu-Zn-Zr catalysts for the CO_2 hydrogenation reaction to methanol, Appl. Catal. B Environ., 152-153 (2014) 152-161.

[15] K.-D. Jung, A.T. Bell, Role of Hydrogen Spillover in Methanol Synthesis over Cu/ZrO_2, J. Catal., 193 (2000) 207-223.

[16] P. Lu, L. Gapu Chizema, E. Hondo, M. Tong, C. Xing, C. Lu, Y. Mei, R. Yang, CO_2 Hydrogenation to Methanol via In- situ Reduced Cu/ZnO Catalyst Prepared by Formic acid Assisted Grinding, ChemistrySelect, 4 (2019) 5667-5677.

[17] I. Kasatkin, P. Kurr, B. Kniep, A. Trunschke, R. Schlogl, Role of Lattice Strain and Defects in Copper Particles on the Activity of Cu/ZnO/Al_2O_3 Catalysts for Methanol Synthesis, Angew. Chem. Int. Ed., 46 (2007) 7324-7327.

[18] P. Lu, E. Hondo, L. Gapu Chizema, C. Lu, Y. Mei, M. Tong, C. Xing, R. Yang, Influence of Tandem Catalysis and Optimised Parameters on Syngas-Dimethyl Ether Co-fed Process for Ethanol Direct Synthesis in a Dual Bed Reactor, Catal. Lett., 149 (2019) 3203-3216.

[19] Q. Ge, Y. Lian, X. Yuan, X. Li, K. Fujimoto, High performance Cu–ZnO/Pd-β catalysts for syngas to LPG, Catal. Commun., 9 (2008) 256-261.

[20] A.Z. Varzaneh, J. Towfighi, A. Mohamadalizadeh, Comparative study of naphtha cracking over SAPO-34 and HZSM-5: Effects of cerium and zirconium on the catalytic performance, J. Anal. Appl. Pyrolysis, 107 (2014) 165-173.

[21] J. Chen, X. Wang, D. Wu, J. Zhang, Q. Ma, X. Gao, X. Lai, H. Xia, S. Fan, T.-S.

Zhao, Hydrogenation of CO_2 to light olefins on CuZnZr@(Zn-)SAPO-34 catalysts: Strategy for product distribution, Fuel, 239 (2019) 44-52.

[22] F. Wang, Z. Wen, Z. Qin, Q. Fang, Q. Ge, Z. Li, J. Sun, G. Li, Manganese cluster induce the control synthesis of RHO- and CHA-type silicoaluminaphosphates for dimethylether to light olefin conversion, Fuel, 244 (2019) 104-109.

[23] S. Soltanali, J.T. Darian, Synthesis of mesoporous SAPO-34 catalysts in the presence of MWCNT, CNF, and GO as hard templates in MTO process, Powder Technol., 355 (2019) 127-134.

[24] Y.-N. Li, X.-F. Liu, L.-N. He, An alternative route of CO_2 conversion: Pd/C-catalyzed oxazolidinone hydrogenation to HCOOH and secondary alkyl-(2-arylethyl)amines with one stone two bird strategy, J. CO_2 Util., 29 (2019) 74-81.

[25] E. Aghaei, M. Haghighi, Z. Pazhohniya, S. Aghamohammadi, One-pot hydrothermal synthesis of nanostructured ZrAPSO-34 powder: Effect of Zr-loading on physicochemical properties and catalytic performance in conversion of methanol to ethylene and propylene, Microporous Mesoporous Mater., 226 (2016) 331-343.

[26] H.J. Kim, J.W. Kim, N. Kim, T.W. Kim, S.H. Jhung, C.U. Kim, Controlling size and acidity of SAPO-34 catalyst for efficient ethylene to propylene transformation, Mol. Catal., 438 (2017) 86-92.

[27] J. Agrell, Production of hydrogen from methanol over Cu/ZnO catalysts promoted by ZrO_2 and Al_2O_3, J. Catal., 219 (2003) 389-403.

[28] A.V. Kirilin, J.F. Dewilde, V. Santos, A. Chojecki, K. Scieranka, A. Malek, Conversion of Synthesis Gas to Light Olefins: Impact of Hydrogenation Activity of Methanol Synthesis Catalyst on the Hybrid Process Selectivity over Cr–Zn and Cu–Zn with SAPO-34, Ind. Eng. Chem. Res., 56 (2017) 13392-13401.

[29] X. Zhu, S. Liu, Y. Song, L. Xu, Catalytic Cracking of C_4 alkenes to propene and ethene: Influences of zeolites pore structures and Si/Al_2 ratios, Appl. Catal. A Gen., 288 (2005) 134-142.

[30] D. Chen, K. Moljord, A. Holmen, A methanol to olefins review: Diffusion, coke formation and deactivation on SAPO type catalysts, Microporous Mesoporous Mater.,

164 (2012) 239-250.

[31] S. Xu, Y. Zhi, J. Han, W. Zhang, X. Wu, T. Sun, Y. Wei, Z. Liu, Advances in Catalysis for Methanol-to-Olefins Conversion, Adv. Catal., 61 (2017) 37-122.

View Article Online
DOI: 10.1039/D0NJ00907E

Graphical Abstract

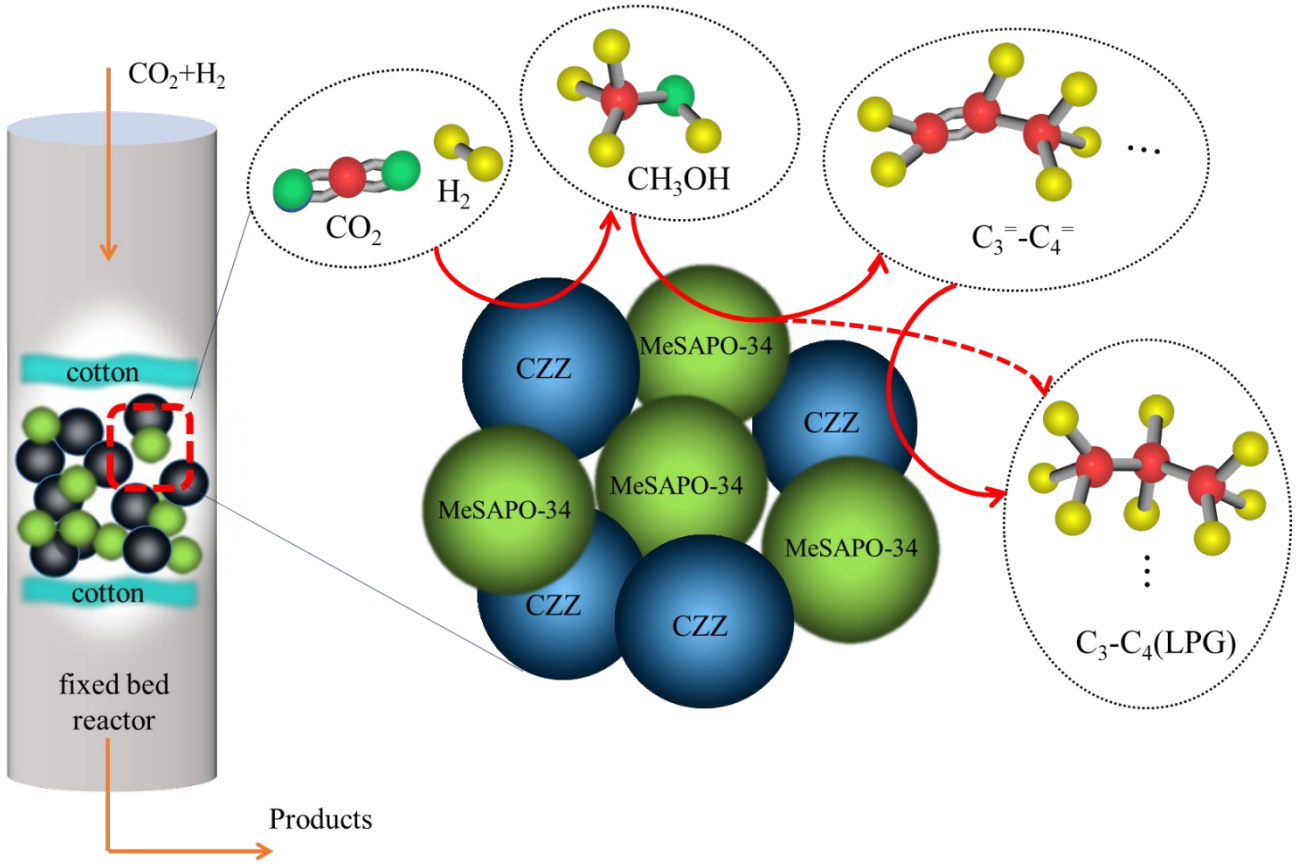

A synergetic relationship established between the metal and modified zeolite components favored higher selectivity for target product (LPG).